

A decorative graphic in the top left corner consists of a 4x4 grid of squares. The colors of the squares transition from dark blue at the bottom-left to light purple at the top-right. The grid is partially cut off by the slide's edge.

Impact of ion diamagnetic drift effect on MHD stability at edge pedestal of rotating tokamaks

N. Aiba, M. Honda, K. Kamiya

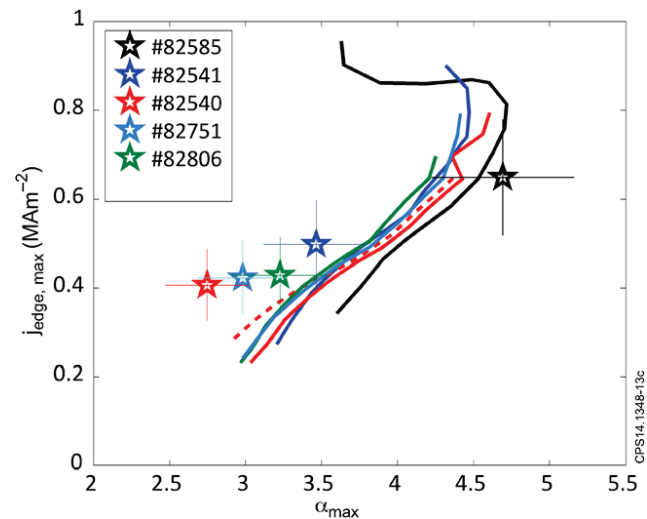
Japan Atomic Energy Agency

Introduction

- Peeling-balloon mode (PBM) is the strongest candidate of the trigger of the type-I edge localized mode (ELM). [Snyder PoP2002 etc.]
- Usually, the toroidal mode number (n) of the mode is intermediate (~ 30), but the results in JT-60U and JET-ILW imply higher- n modes sometimes trigger type-I ELM. [Aiba NF2011, Giroud PPCF2015]
- Theoretically, such high- n modes are stabilized by an ion diamagnetic drift (ω_{*i}) effect.[Tang NF1980 etc.]

What causes the discrepancy between theory and experiment?

→ Rotation is a candidate of the key parameter.



PBM stability diagram in JET-ILW (n is up to 50), [Giroud PPCF2015]

Drift MHD model

To analyze the PBM stability with ω_{*i} effect in rotating plasmas, we use the drift MHD model derived by Hazeltine and Meiss.
 [Hazeltine and Meiss, Plasma Confinement]

$$\frac{DN}{Dt} + N\nabla \cdot \mathbf{V} = 0, \quad \left. \frac{DP}{Dt} \right|_{MHD} + \Gamma P \nabla \cdot \mathbf{V}_{MHD} = 0,$$

$$\mathbf{E} + \mathbf{V}_{MHD} \times \mathbf{B} + \frac{1}{eN} \nabla P = 0, \quad m_i N \left(\left. \frac{D\mathbf{V}_E}{Dt} + \frac{D}{Dt} \right|_{MHD} (\mathbf{V}_{\parallel} \mathbf{b}) \right) = \mathbf{J} \times \mathbf{B} - \nabla P.$$

$$\mathbf{V} = \mathbf{V}_{MHD} + \mathbf{V}_{pi} = \mathbf{V}_E + \mathbf{V}_{\parallel} \mathbf{b}, \quad \mathbf{V}_{pi} = \frac{\mathbf{B} \times \nabla p_i}{eZN\mathbf{B}^2}, \quad \mathbf{V}_E = \frac{\mathbf{E} \times \mathbf{B}}{\mathbf{B}^2},$$

$$\frac{D}{Dt} = \frac{\partial}{\partial t} + (\mathbf{V} \cdot \nabla), \quad \left. \frac{D}{Dt} \right|_{MHD} = \frac{\partial}{\partial t} + (\mathbf{V}_{MHD} \cdot \nabla)$$

N : number density, \mathbf{V} : velocity, P : pressure, Γ : heat capacity ratio,

\mathbf{E} : electric field, \mathbf{B} : magnetic field, \mathbf{J} : plasma current, $\mathbf{b} \equiv \mathbf{B}/B$,

e : elementary charge, m_i : ion mass, Z : effective charge, p_i : ion pressure

Approximations used for simplifying the drift MHD model

We simplify the model with Frieman-Rotenberg formalism.

Approximations:

1. In Faraday's law, non-ideal term is neglected.

$$\frac{\partial \mathbf{B}}{\partial t} = \nabla \times \mathbf{E} = -\nabla \times \left(\mathbf{V}_{MHD} \times \mathbf{B} + \frac{1}{eN} \nabla P \right)$$

This approximation can be justified when

- a. Rotation is enough slow compared to ion thermal velocity.
- b. Density N or temperature T is constant in a plasma
- c. Functional form of N is proportional to that of T .

(Details are in Appendix)

2. Magnetic field varies slowly $\nabla \times (\mathbf{b}/B) \ll 1$.

This helps to change the continuity equation as follows.

$$\left. \frac{DN}{Dt} \right|_{MHD} + N \nabla \cdot \mathbf{V}_{MHD} = 0$$

Simplified drift MHD equation

Also, by assuming the incompressibility $\nabla \cdot \xi = 0$, the flute approximation $(\mathbf{B} \cdot \nabla) \xi \ll 1$ and $T_i = T_e$, we can derive the following equation [Aiba submitted to PPCF].
 $(T_i(T_e)$: ion (electron) temperature).

$$\begin{aligned} \rho_0 \frac{\partial^2 \xi}{\partial t^2} + 2\rho_0 (\mathbf{V}_{0,MHD} \cdot \nabla) \frac{\partial \xi}{\partial t} + \rho_0 (\mathbf{V}_{0,pi} \cdot \nabla) \frac{\partial \xi_{\perp}}{\partial t} &= \mathbf{F}_{MHD} + \mathbf{F}_{di}, \\ \mathbf{F}_{MHD} &= \mathbf{J}_0 \times \mathbf{B}_1 + (\nabla \times \mathbf{B}_1) \times \mathbf{B}_0 - \nabla P_1 \\ &\quad + \nabla \otimes [\rho_0 \xi \otimes (\mathbf{V}_0 \cdot \nabla) \mathbf{V}_{0,MHD} - \rho_0 \mathbf{V}_0 \otimes (\mathbf{V}_{0,MHD} \cdot \nabla) \xi], \\ \mathbf{F}_{di} &= \rho_0 \frac{\nabla \cdot (\xi \times \nabla P_0)}{2en_0 B_0^2} (\mathbf{B}_0 \cdot \nabla) \mathbf{V}_{0,MHD,\perp}, \\ \nabla \cdot \xi &= 0, \quad \mathbf{V}_0 = \mathbf{V}_{0,MHD} + \mathbf{V}_{0,pi}, \quad \mathbf{V}_{0,pi} = \frac{1}{2eZn_0 B_0^2} \mathbf{B}_0 \times \nabla P_0 \end{aligned}$$

MINERVA code[Aiba CPC2009] is updated to solve this equation.



MINERVA-DI code

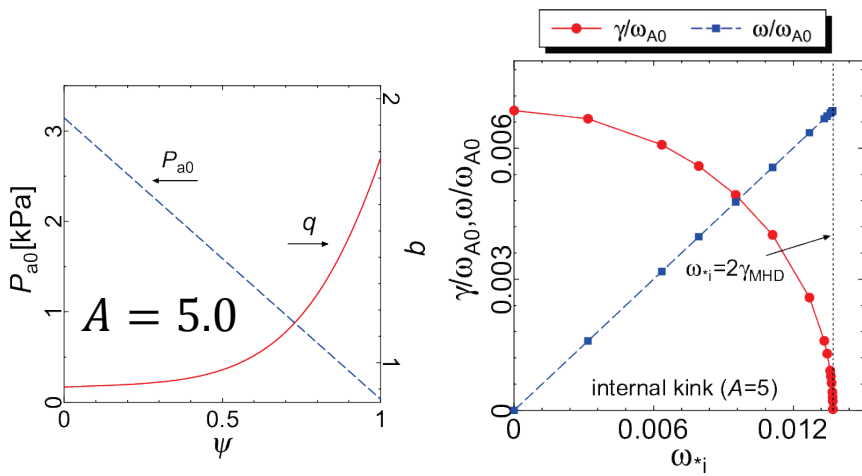
Benchmark test of MINERVA-DI

In a static plasma, the growth rate γ and the mode frequency ω can be estimated by the dispersion relation with ω_{*i} ($= \mathbf{k} \cdot \mathbf{V}_{0,pi}$) effect as follows.[Tang NF1980 etc.]

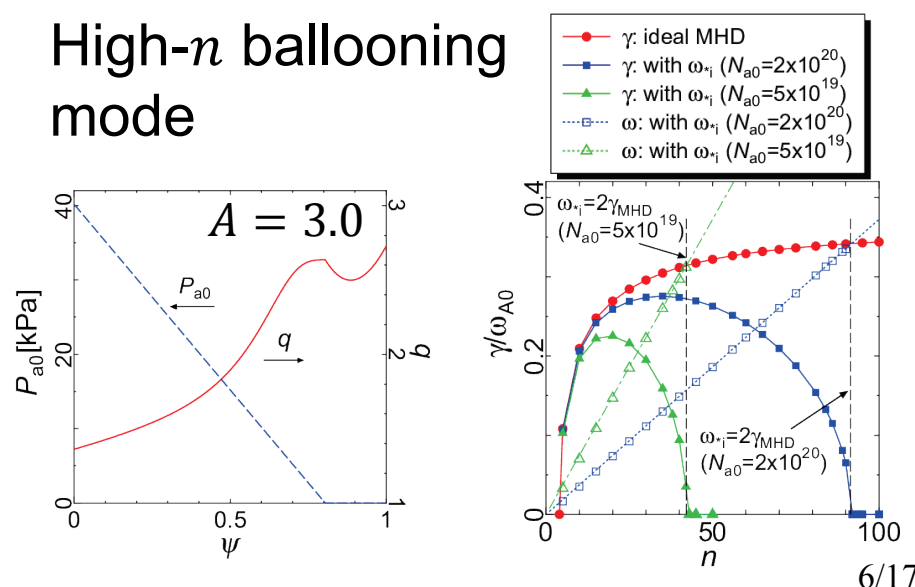
$$\gamma + i\omega = \frac{i\omega_{*i}}{2} \pm \sqrt{\gamma_{MHD}^2 - \frac{\omega_{*i}^2}{4}}, \quad \gamma_{MHD}: \gamma \text{ of ideal MHD mode}$$

MINERVA-DI shows good agreements with this when internal kink and high- n ballooning stability is analyzed.

Internal kink mode ($n = 1$)



High- n ballooning mode

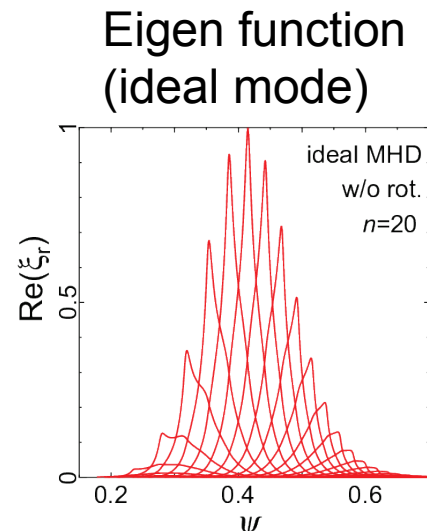
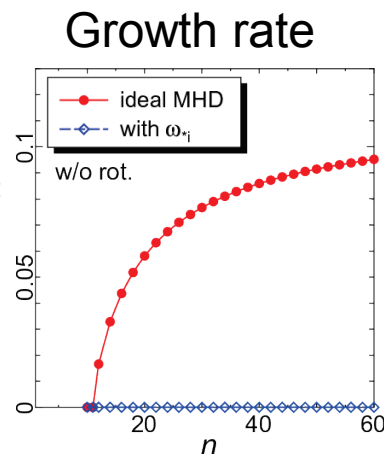
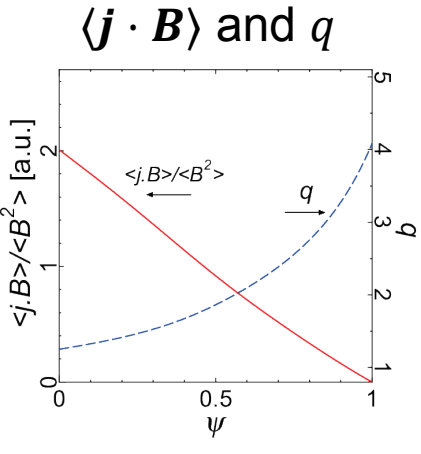
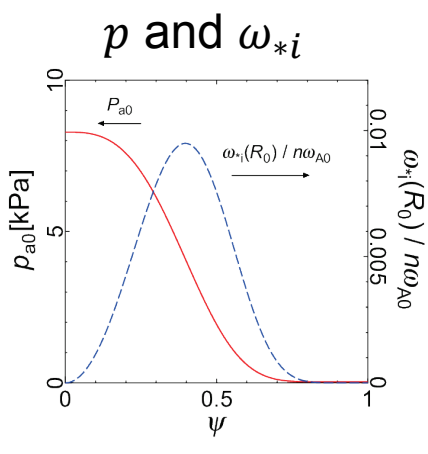


Ballooning mode stability with ω_{*i} is analyzed in rotating tokamaks

- Equilibrium has circular cross-section, and $A = 3.0$.
- Ideal ballooning mode is unstable for $n \geq 12$, but the mode is suppressed by ω_{*i} effect.
- Plasma (hydrogen) density is $N = 2.0 \times 10^{19} [1/m^3]$.
- Rotation profile is determined as follow.

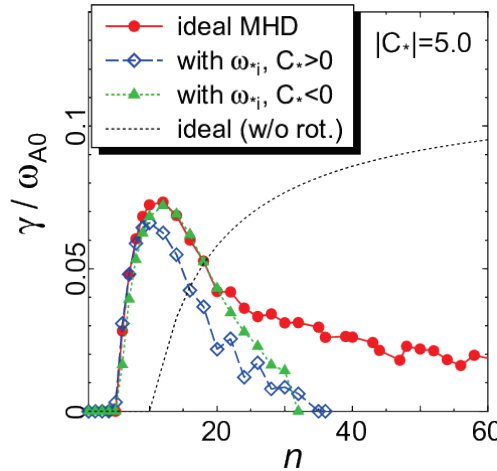
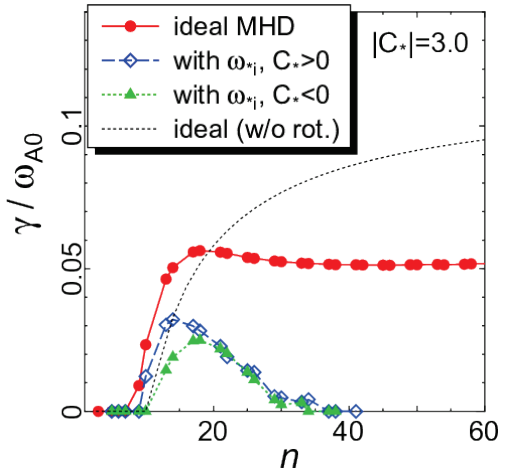
$$\begin{aligned}\Omega_\phi &= C_* \omega_{*,i,peak} \quad (0 \leq \psi \leq \psi_{peak}) \\ &= C_* \omega_{*,i}(\psi, R_0) \quad (\psi_{peak} \leq \psi \leq 1)\end{aligned}$$

Here $\omega_{*,i,peak} = 9.51 \times 10^{-3} \omega_{A0}$ at $\psi = \psi_{peak}$, ω_{A0} is the toroidal Alfvén frequency on axis.

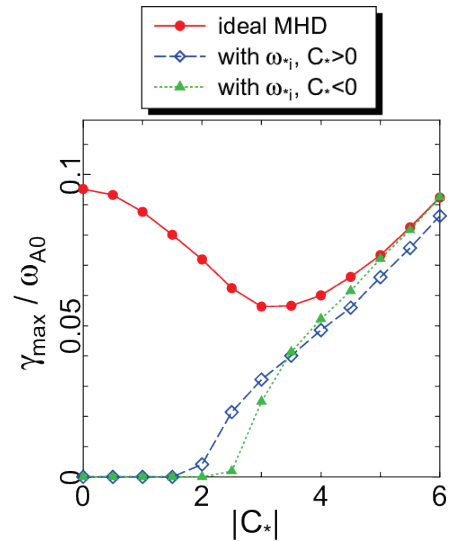


Plasma rotation can cancel ω_{*i} stabilizing effect on ballooning mode

Dependence of γ on n (left: $|C_*| = 3.0$, right: $|C_*| = 5.0$)



Dependence of γ on $|C_*$

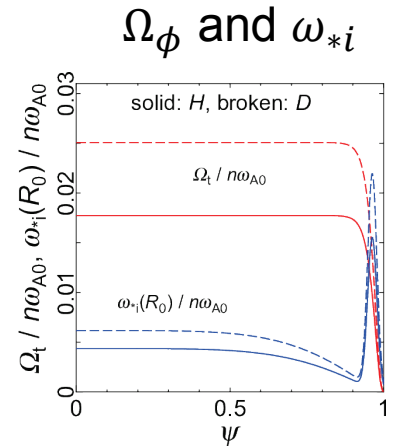
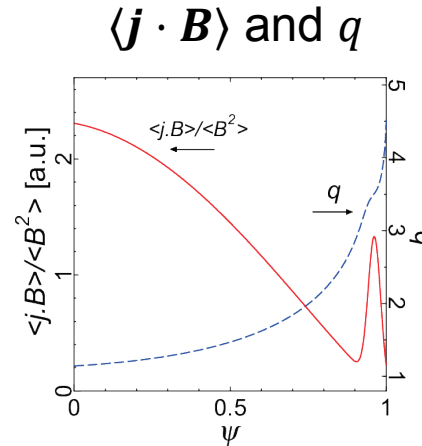
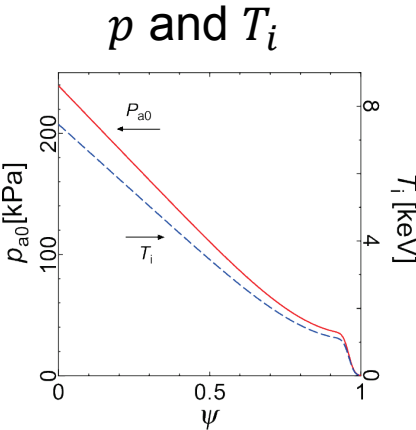
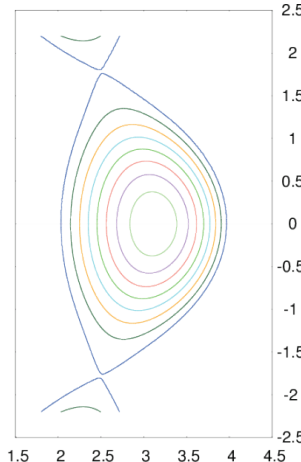


Plasma rotation changes ballooning mode stability as follows.

- Intermediate- n modes become unstable, though high- n modes are stabilized.
- Ballooning mode becomes unstable even when ω_{*i} effect is taken into account.
- Maximum γ of ballooning mode with ω_{*i} effect is converged to that of ideal ballooning mode.

PBM stability with ω_{*i} is analyzed in a rotating shaped tokamak

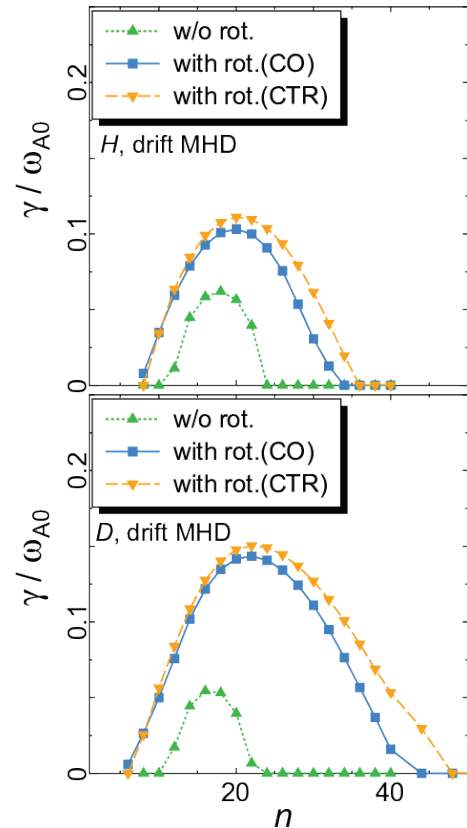
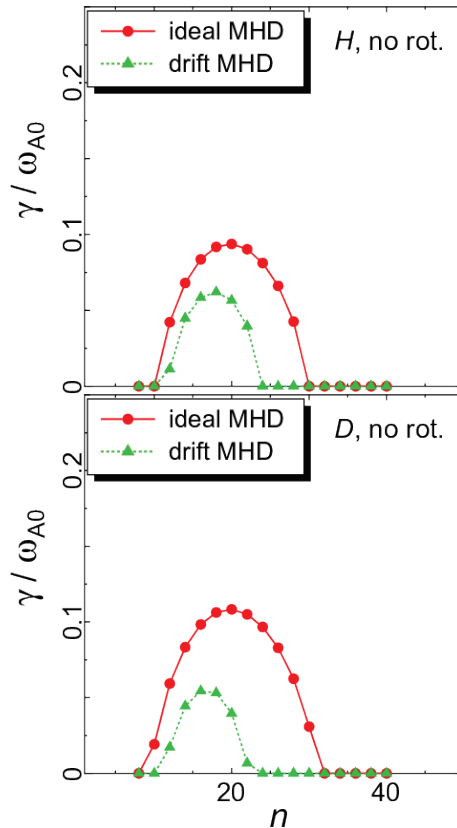
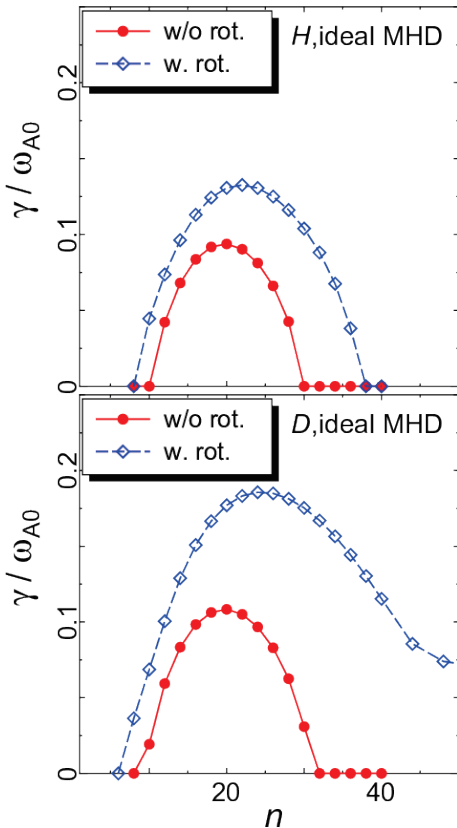
Contours of ψ



- PBM stability is analyzed in D-shaped (double-null) plasma.
- Density is assumed as $N = 1.0 \times 10^{20} [1/m^3]$.
- Rotation profile is determined as follow.
$$\Omega_\phi [\text{krad/s}] = 49.5(1 - \psi^{48})^4 + 0.5.$$
- By changing bulk ion species from hydrogen H to deuterium D , $\Omega_\phi / \omega_{A0}$ and $\omega_{*i} / \omega_{A0}$ is increased by factor of $\sqrt{2}$.
- PBM stability is analyzed in both H and D plasmas.

Rotation of “heavy” plasma has large impact on PBM stability

Results in
 H plasma



Results in
 D plasma

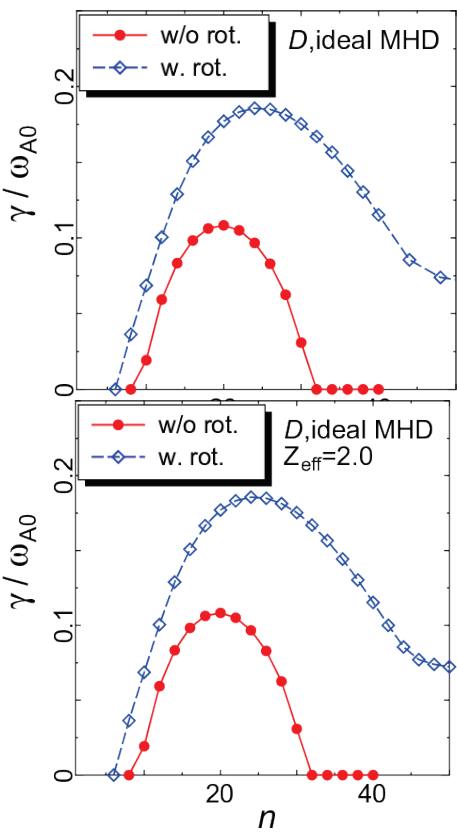
Large $\Omega_\phi / \omega_{A0}$ has impact on PBM stability, but impact of ω_{*i} on PBM is not affected by ion species so much,



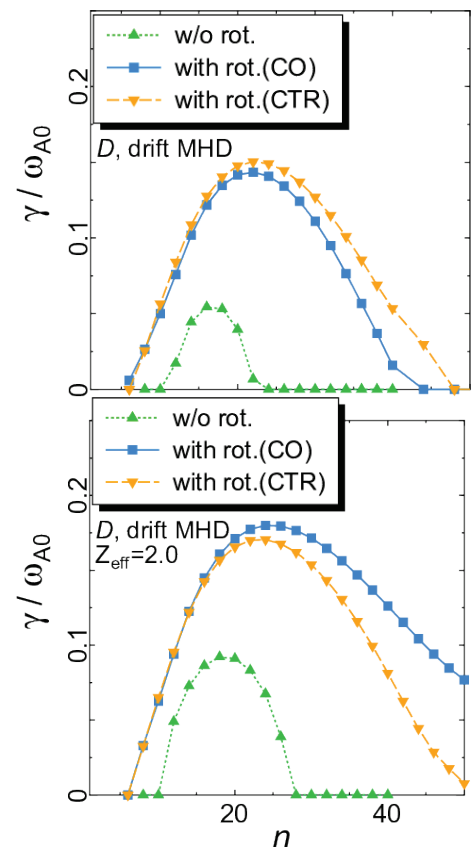
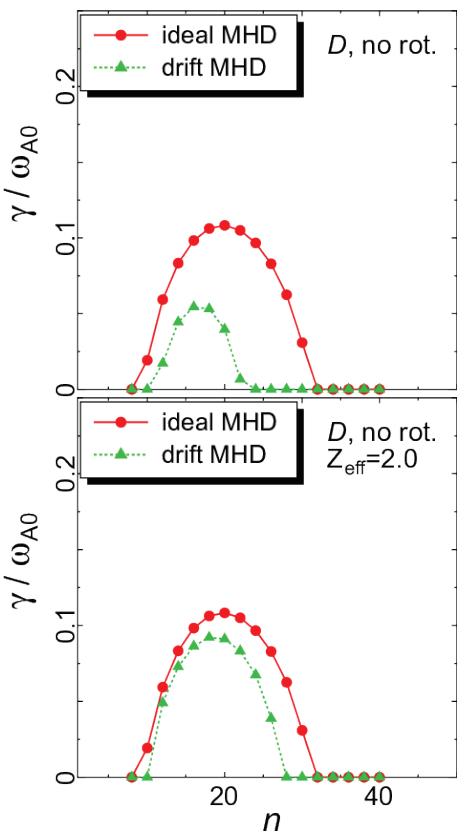
Plasma effective mass potentially changes (ideal) PBM stability.

Large Z_{eff} reduces impact of ω_{*i} on PBM stability

Results in
 D plasma
($Z_{eff} = 1.0$)



Results in
 D plasma
($Z_{eff} = 2.0$)



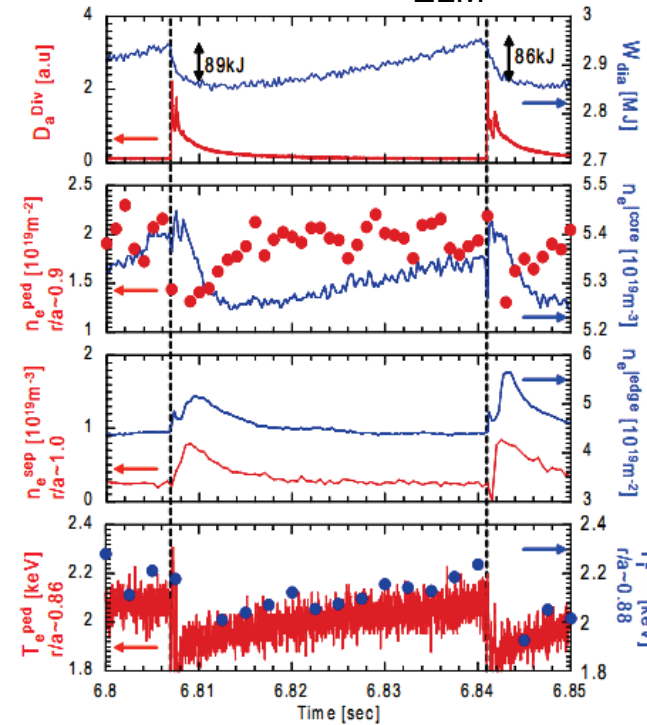
Impact of ω_{*i} on PBM stability depends on Z_{eff} due to $\omega_{*i} \propto Z_{eff}^{-1}$, but ideal MHD stability is independent from Z_{eff} .

→ Plasma effective charge changes ω_{*i} effect on PBM stability.

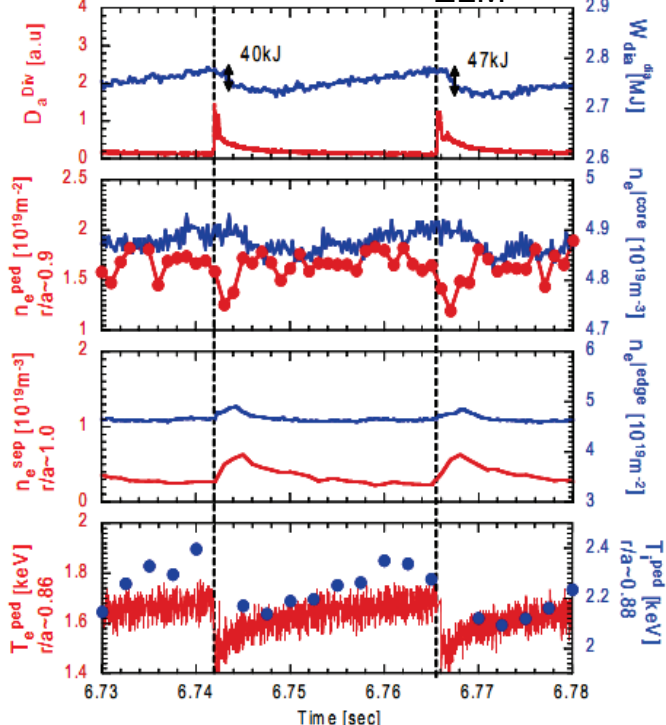
Rotation effect on type-I ELM in JT-60U

The equilibria analyzed numerically are E49228 and E49229; these are type-I ELMy H-mode plasmas [A. Kojima et al., NF, (2009)].

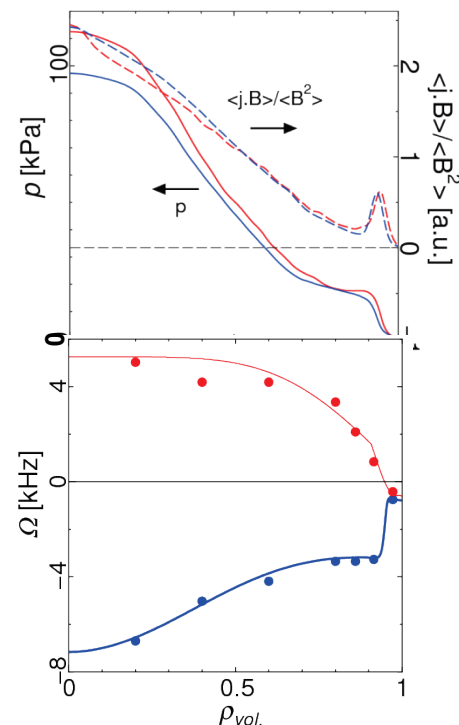
E49228 (CO.) $f_{\text{ELM}} \sim 37 \text{ Hz}$



E49229 (CTR.) $f_{\text{ELM}} \sim 45 \text{ Hz}$



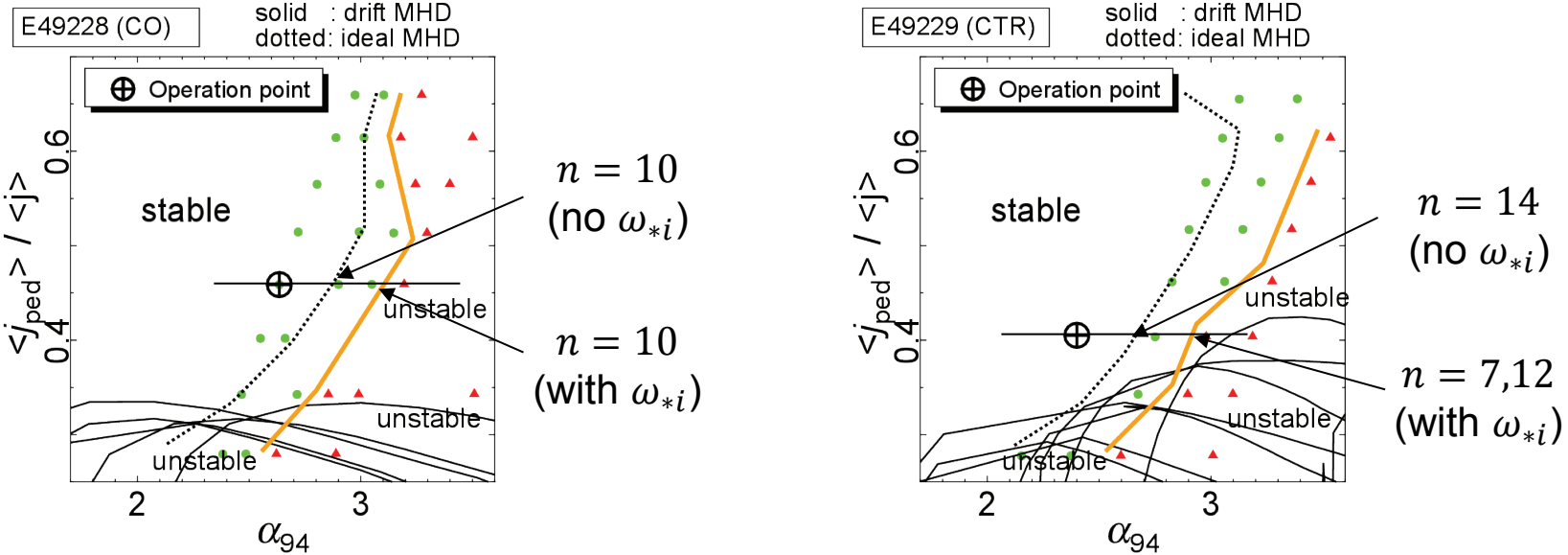
Profiles of $p, j \cdot B, \Omega$



We compare the results of the numerical stability analysis of these equilibria just before ELM.

Stability boundary is shifted by ω_{*i} effect in static plasmas

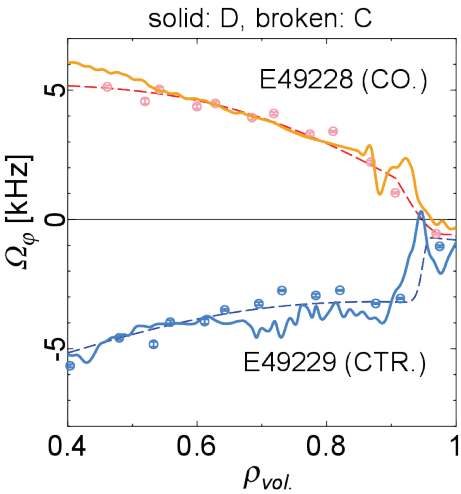
$\langle j_{ped} \rangle - \alpha_{94}$ diagram ($Z_{\text{eff}} = 2.0$) (left:CO., right CTR.)



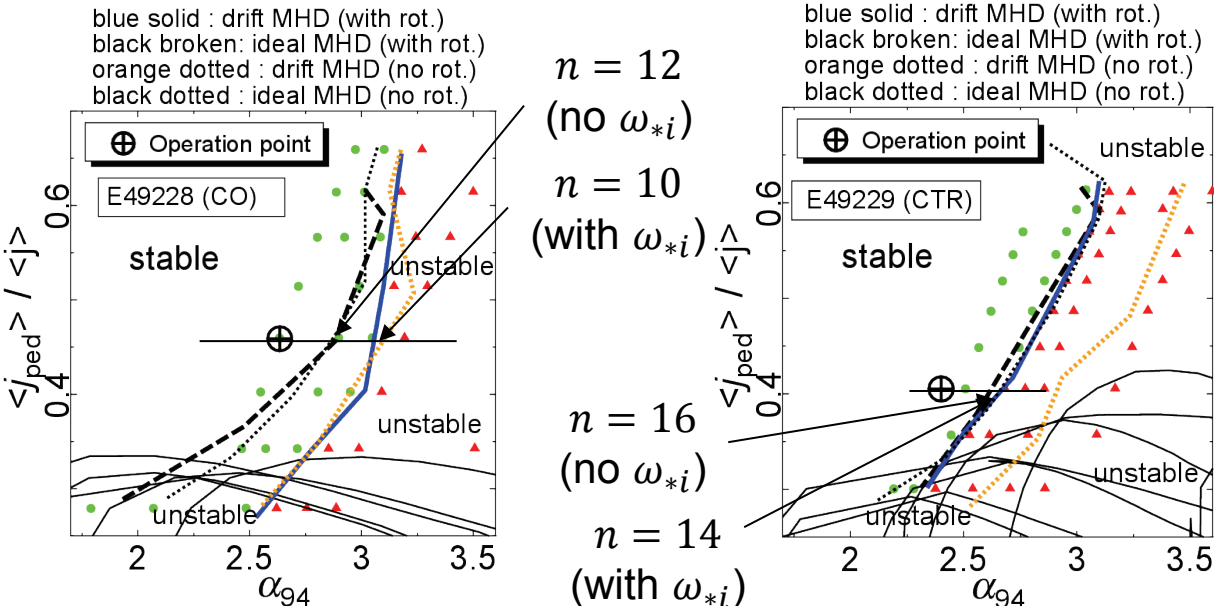
- When the plasma is assumed as static, PBM stability boundary is shifted to larger- α side by ω_{*i} effect as expected.
- Difference between operation point and boundary increases from $\sim 10\%$ to $> 20\%$ of α_{94} on operation point in E49228, and from $\sim 20\%$ to $\sim 40\%$ in E49229.

Plasma rotation can counteract ω_{*i} effect on PBM stability boundary

Ω_ϕ of C and D



$\langle j_{ped} \rangle - \alpha_{94}$ diagram ($Z_{\text{eff}} = 2.0$) (left: CO., right CTR.)



- Rotation profile of deuterium (D) is estimated with TOPICS integrated simulation code. [M. Honda NF2013]
- Rotation has little impact on pedestal stability in E49228.
- Rotation cancels ω_{*i} effect on pedestal stability in E49229, but the stability boundary is still far from operation point.



Poloidal rotation can affect edge MHD stability

Difference of the mode frequency $n\omega$ from the Doppler-shifted frequency $\mathbf{k} \cdot \mathbf{v}$ is essential for destabilizing edge MHD modes.[Aiba NF2011].

$$\mathbf{k} \cdot \mathbf{v} = -in\Omega_\phi + im\Omega_\theta \quad \Omega_\phi : \text{toroidal rotation freq., } \Omega_\theta : \text{poloidal rotation freq.}$$

n : toroidal mode number, m : poloidal mode number

For the Fourier harmonics which satisfy $m-nq=0$, $m\Omega_\theta \sim n\Omega_\phi$ even when $v_\theta = (nr/mR)v_\phi \sim 0.1v_\phi$ if $q=3$ and $R/r \sim 3.3$.

$$= i\Omega_{\parallel}(\mathbf{k} \cdot \mathbf{B}/B) - in\Omega_t \quad \Omega_{\parallel} : \text{freq. parallel to magnetic field,}$$

Ω_t : freq. in toroidal direction

Near rational surfaces, $\mathbf{k} \cdot \mathbf{B} \sim 0$. $\rightarrow \Omega_t$ will be important.

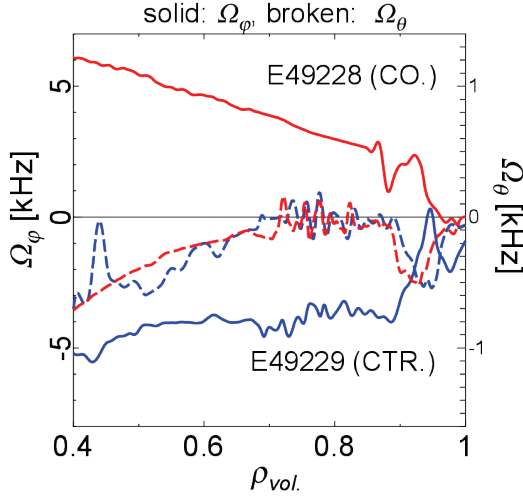
MINERVA(-DI) can identify the poloidal rotation effect on MHD stability (at present, poloidal rotation effect on equilibrium is neglected.)



Re-evaluate stability diagram with not only Ω_ϕ but also Ω_θ .

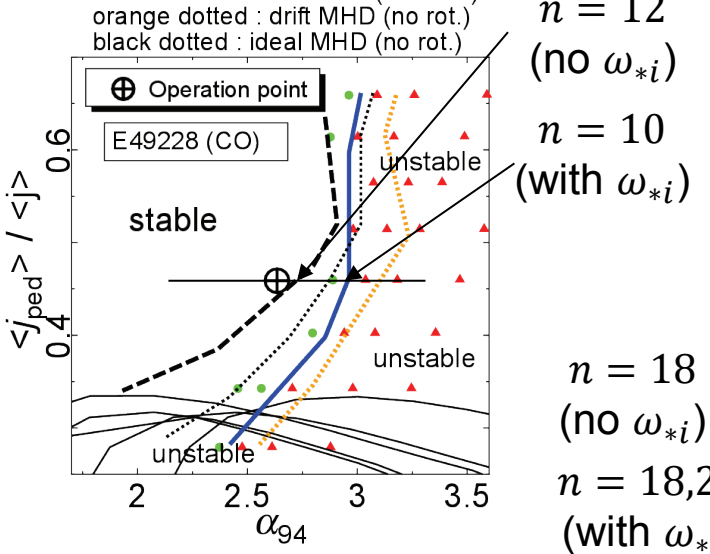
PBM stability boundary can be predicted by counting Ω_ϕ and Ω_θ

Ω_ϕ and Ω_θ of D



$\langle j_{ped} \rangle - \alpha_{94}$ diagram ($Z_{eff} = 2.0$) (left:CO., right CTR.)

blue solid : drift MHD (with rot.)
 black broken: ideal MHD (with rot.)
 orange dotted : drift MHD (no rot.)
 black dotted : ideal MHD (no rot.)

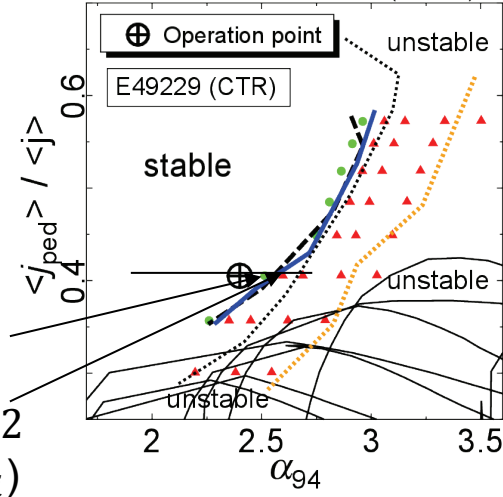


$n = 12$
 (no ω_{*i})

$n = 10$
 (with ω_{*i})

$n = 18$
 (no ω_{*i})
 $n = 18,22$
 (with ω_{*i})

blue solid : drift MHD (with rot.)
 black broken: ideal MHD (with rot.)
 orange dotted : drift MHD (no rot.)
 black dotted : ideal MHD (no rot.)



- In E49228, poloidal (+toroidal) rotation moves the ideal MHD boundary near operation point, but ω_{*i} effect shifts the boundary far from the point.
- In E49229, ω_{*i} effect is negligible as the toroidally rotating case, and the boundary becomes closer operation point.

Summary

- Linearized drift MHD equation was derived with Frieman-Rotenberg formalism.
- MINERVA-DI code was developed to solve the drift MHD equation.
- It is found that ion diamagnetic drift (ω_{*i}) effect on ballooning/peeling-balloonning(PBM) stability can be canceled by plasma rotation.
- Effective mass/charge have potential to change PBM stability when rotation and ω_{*i} are counted.
- Cancellation of ω_{*i} effect by rotation plays an important role on PBM stability boundary in JT-60U.
- PBM stability analysis in JET ITER-like metallic wall is on going, and the result will be reported in near future.